Spin-diffusion coefficient in gaseous helium between 1 and 0.5 K

M. Himbert, J. Dupont-Roc, and C. Lhuillier*
Laboratoire de Spectroscopie Hertzienne de l'Ecole Normale Supérieure, 24 rue Lhomond, 75231 Paris CEDEX 05, France
(Received 2 December 1988)

We report on measurements of the nuclear-spin diffusion coefficient in gaseous helium below 1 K. Both D_{33} (self-diffusion in ^{3}He) and D_{34} (diffusion of ^{3}He in ^{4}He) are obtained from T_2 measurements in applied magnetic gradients. We operate at low densities, where transport properties are governed by two-body collisions. Predictions from various helium-helium potentials have been computed and are compared with the experimental results. A rough agreement is obtained, although theoretical values for D_{33} seem somewhat too small. Relative variations with temperature are well described by theory between 4.2 and 0.5 K (within 10%).

I. INTRODUCTION

Transport properties of polarized ^{3}He gas have recently been investigated in detail both from theoretical[1] and experimental[2] points of view because, as a consequence of the Pauli principle, the introduction of a nuclear polarization modifies drastically the low-temperature transport phenomena. More traditionally, transport coefficients are used as sensitive tests for proposed He-He pair potentials. The transport theory for gases is well established,[1,3] and precise computations of the transport coefficients for various potentials are feasible.

Considerable efforts have been made to produce accurate pair potential for helium atoms. *Ab initio* calculations[4] are mostly relevant to the repulsive part or the long-range part of the interaction potential. To bridge the gap between these two regions, sophisticated model potentials have been constructed by adjustment to the thermodynamical and the transport properties of the helium gas,[5-7] or have been extracted from scattering data.[8] Most recent *ab initio* computations are now also starting to be competitive in the intermediate region.[9]

On the experimental side, although low-energy or low-temperature data have been recognized as highly discriminating for proposed potentials, especially for the well region,[10] very little information is available. The lowest energy in scattering experiments is higher than 1.5 K (Ref. 8) and the transport data used by Aziz *et al.*[6,7] have been taken above 1.3 K. Only the second virial coefficient was recently measured down to 0.63 K.[11]

We report here on a measurement by NMR techniques of the ^{3}He spin-diffusion coefficient in pure ^{3}He and in ^{3}He-^{4}He gas mixtures, in the temperature range from 1 to 0.5 K. Comparison is made with theoretical predictions based on different potentials: the standard Lennard-Jones (LJ) potential,[5] and composite potentials built with a Hartree-Fock repulsive part empirically joined to a dispersive long-distance attraction, proposed by Aziz and co-workers[6,7] and Feltgen *et al.*[8] denoted as HFDHE2 (Ref. 6), HFD-B(HE) (Ref. 7), and HFIMD (Ref. 8). Detailed information on these potentials is given in Appendix A.

Previously, the spin-diffusion coefficient D_{34} was measured by Bendt[12] down to 1.74 K and at higher temperature by others.[13-15] The self-diffusion coefficient D_{33} was measured down to 1 K by Luszczynski *et al.*[16] and also by Barbé[17] at 4.2 K. More recently, Nacher and coworkers obtained both D_{33} and D_{34} from 4 to 1.3 K as a by-product of their spin-wave experiments.[18,19]

II. EXPERIMENTAL METHODS

We consider here densities n of the order of 10^{16} cm^{-3}. The de Broglie wavelength λ is of the order of (10 Å/$\sqrt{T}$) for ^{3}He, so that the condition $n\lambda^3 \ll 1$ is fulfilled. The Boltzmann statistics can be used to describe the gas. Furthermore, if we note a to be a typical range for the He-He potential at low energy (a few angstroms), the inequality $na^3 \ll 1$ is fulfilled and thus binary collisions dominate the transport properties. We consider also weak spin-polarization, so that identical spin-rotation effects are negligible.[1] In that limit, a ^{3}He-^{4}He mixture behaves like a three-component classical mixture[20,21] with densities n_3^+, n_3^-, and n_4. In presence of ^{4}He, the spin-up and spin-down ^{3}He gases diffuse through each other with a diffusion coefficient D given by

$$\frac{1}{D} = \frac{n_3}{nD_{33}} + \frac{n_4}{nD_{34}} , \tag{1}$$

where $n_3 = n_3^+ + n_3^-$ and $n = n_3 + n_4$ are particle densities and where

$$\frac{1}{nD_{ij}} \simeq \tfrac{16}{3}\mu_{ij}\frac{\Omega_{ij}^{(1,1)}}{k_B T} . \tag{2}$$

The collision integral $\Omega_{ij}^{(1,1)}$ depends on the pair potential and on the temperature T [μ_{ij} is the reduced mass in a two-body collision between i and j ($i,j=3$ or 4)].[22]

Measurements of D^{-1} for various ^{3}He-^{4}He mixtures yield $(nD_{33})^{-1}$ and $(nD_{34})^{-1}$ through Eq. (1).

The ^{3}He-^{4}He mixture is contained in spherical Pyrex cells, 3 cm in diameter. The gas densities, ranging from 10^{16} to 10^{18} cm^{-3}, are accurately measured during the filling procedure. Cells are sealed[23] at room temperature, then cooled down to 0.5 K by a ^{3}He refrigerator, to

which the cell is thermalized by a superfluid helium bath. Temperature is monitored by a Ge resistor, calibrated versus ^{3}He vapor pressure. The estimated accuracy is of the order of 20 mK. Nuclear orientation is obtained by optical pumping,[24] performed directly at low temperature.[25] Part of the ^{4}He gas is condensed on the Pyrex walls of the cell and acts as a coating to prevent strong wall relaxation of ^{3}He nuclear spins.[26] This technique gives a polarization of the order of 3%. A static magnetic field B_0 (1.4×10^{-3} T, Larmor frequency of the order of 45 kHz) keeps the polarization along the z direction.

The spin-diffusion coefficient D is deduced from measurements of the relaxation time T_2 (transverse magnetization relaxation time) in controlled field gradients. More precisely, linear gradients are applied by a set of Helmholtz coils connected in opposition. The amplitude δB_z of the total field variation over the cell is low enough so that motional averaging can take place during the spin diffusion time τ_D ($\gamma\delta B_z\tau_D \ll 1$).[27] Under these conditions, the applied gradients result in an additional relaxation rate Γ_m:

$$\frac{1}{T_2}=\frac{1}{T_2^0}+\Gamma_m \ , \tag{3}$$

where $1/T_2^0$ is independent of the applied gradient. The induced relaxation rate Γ_m is related to the spin-diffusion coefficient by the following formula:[28]

$$\Gamma_m=4.57\times10^{-2}(\gamma\nabla B_z)^2\frac{R^4}{D} \ , \tag{4}$$

where R is the cell radius and γ the gyromagnetic ratio of ^{3}He.

Experimentally, T_2 is measured at fixed temperature by monitoring the decay of the transverse polarization after a $\pi/2$ pulse for various values of ∇B_z. A parabola is adjusted by a least-squares fit to the values of $1/T_2$ versus $|\nabla B_z|$, and D is deduced with the help of (4).

III. ABSOLUTE VALUE OF nD_{33} AT 0.57 K

The values of $1/D$ are measured as described above for a set of identical cells filled at 300 K with a ^{3}He density increasing from n_0 to $3n_0$, n_0 being a reference value corresponding to a 1 Torr at 300 K, i.e.,

$$n_0\simeq3.22\times10^{16}\ \text{cm}^{-3} \ . \tag{5}$$

The amount of ^{4}He added in these samples at 300 K corresponds to a density higher than $2n_0$. Accordingly, the ^{4}He gas is under saturated-vapor conditions at $T=0.57$ K, and the gaseous ^{4}He density is taken as $n_4^{\rm SVP}(0.57\ \text{K})=0.07n_0$ (where the superscript SVP denotes the quantity at saturated vapor pressure). The ^{3}He atoms remain almost entirely in the gaseous phase, only 1% or 2% being adsorbed on the ^{4}He film or dissolved in it. This small amount is evaluated assuming a binding energy of 5 K for ^{3}He on the surface of ^{4}He, and 2.8 K inside the film.[29]

The results are presented in Fig. 1, where the solid line is the best linear fit to the experimental points. Its slope gives $n_0(nD_{33})^{-1}$ and the value for $n_3=0$ gives

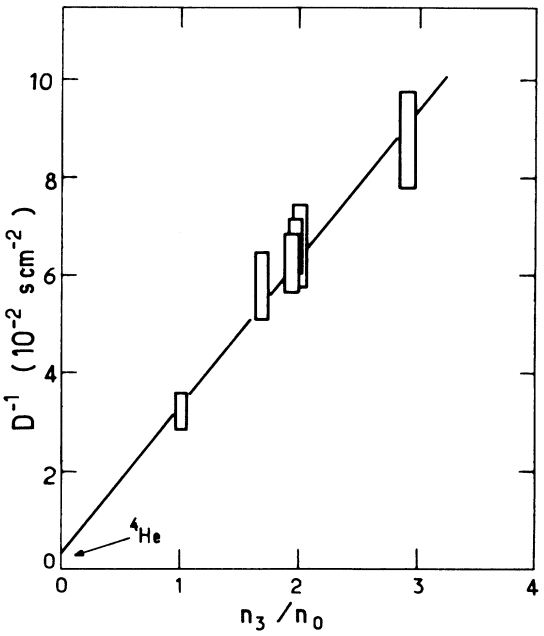

FIG. 1. Linear variation of the spin-diffusion coefficient D^{-1} at 0.57 K with the ^{3}He density n_3, according to (1). n_0 is defined by (5). The ^{3}He-^{4}He mixture gas in the different samples contains the same ^{4}He density, $n_4^{\rm SVP}$. The slope of the solid line, which is a linear least-squares fit to the points, gives $(nD_{33})^{-1}$. The value at $n_3=0$ gives the contribution of ^{4}He.

$n_4^{\rm SVP}(nD_{34})^{-1}$, according to (1). In this way we obtain for $(nD_{33})^{-1}$ at 0.57 K

$$[nD_{33}(0.57\ \text{K})]^{-1}=(0.92\pm0.17)\times10^{-18}\ \text{cm s} \ . \tag{6}$$

It must be stressed that the calibration of the various parameters entering formula (4) is not so easy. The uncertainty comes mainly from the gradient calibration and the determination of the inner radius R of the cell, which appears as R^4 in formula (4). R has been measured in various ways: weighting the cell filled with distilled water, measuring the Pyrex thickness with an optical apparatus, and cutting the cell for direct length determination. All techniques gave consistent results. The rms dispersion on R is about 2.5%, and this value includes deviation of the cell from perfect sphericity.

The field gradient is created by a pair of coils connected in opposition. The calibration versus the dc current in the coils, which is the experimentally monitored parameter, has been made *in situ* by inversing the current in one coil and by measuring the induced shift of the spin Larmor frequency. The final precision for the calibration, involving a few geometrical parameters and including a possible distortion of the gradient field by supraconducting or weakly magnetic materials of the setup, reaches 4%. Other contributions to the experimental error are of less importance. For instance, adsorption of ^{3}He on the ^{4}He film results in a modification of the diffusion of the ^{3}He atoms through the cell. However, at 0.56 K, the proportion of ^{3}He adsorbed is of the order of 0.5%, and this

gives only a slight modification of D^{-1}, which has been taken into account.

IV. RELATIVE VARIATION OF $(nD_{33})^{-1}$ FROM 0.56 K TO HIGHER TEMPERATURES

The preceding discussion suggests that the variation of the diffusion coefficient with the temperature can be obtained with a smaller uncertainty than its absolute value. If the same cell is used at different temperatures, in the same position with respect to the coils producing the linear gradient, the relative variations of the induced relaxation rate $\Gamma_m(T)$ are exactly equal to those of D^{-1}:

$$\frac{\Gamma_m(T)}{\Gamma_m(T_0)}=\frac{[D(T)]^{-1}}{[D(T_0)]^{-1}} . \tag{7}$$

Absolute calibration of the gradient is no longer necessary, neither is precise knowledge of the cell shape. Two parabolic fits of Γ_m versus the current intensity in the gradient coils, achieved for data taken at T and T_0, give directly the experimental values of (7). We measured in this way the ratio of the values of D^{-1} between 0.56 and 4.2 K, and also between 0.56 and 300 K.

The dependence of $D^{-1}(T)$ on T comes from the variation of $(nD_{33})^{-1}$ and $(nD_{34})^{-1}$ with the temperature, and also from the change of the vapor composition due to the partial liquefaction of ^{4}He at 0.56 K. For these particular experiments we used cells filled with a ^{3}He density equal to $1.97n_0$, and a ^{4}He density equal to $0.98n_0$.

A. Variation of D^{-1} from 0.56 to 4.2 K

In this case, the cell contained also a given amount of molecular hydrogen to provide a wall coating at 4.2 K, a temperature at which ^{4}He is not condensed on the walls. Hence both ^{3}He and ^{4}He are in the vapor phase. At 0.56 K (1.80 K^{-1}), the ^{4}He density is the saturated-vapor density, which is $0.05n_0$. Hence the quantity measured experimentally is

$$\frac{[D(0.56\ \mathrm{K})]^{-1}}{[D(4.2\ \mathrm{K})]^{-1}} = \frac{1.96[nD_{33}(0.56\ \mathrm{K})]^{-1}+0.05[nD_{34}(0.56\ \mathrm{K})]^{-1}}{1.97[nD_{33}(4.2\ \mathrm{K})]^{-1}+0.98[nD_{34}(4.2\ \mathrm{K})]^{-1}} . \tag{8}$$

The difference in ^{3}He densities between 0.56 and 4.2 K (1.96 instead of 1.97) is due to the absorption of ^{3}He on and in ^{4}He.

Comparison of the experimental value obtained for (8) with the same quantity computed from various potentials is made in Table I. The "error bar" on the theoretical predictions accounts for the uncertainty on the filling densities, for the temperature uncertainty at 0.56 K which affects the ^{4}He saturated vapor density, and also for the slight modification of the diffusion in the cell due to the small fraction of adsorbed helium atoms.

We noticed that, for all the theoretical potentials used, the quantity

$$q(T)=[nD_{34}(T)]^{-1}/[nD_{33}(T)]^{-1}$$

is nearly potential independent, starting from the classical value $(\frac{8}{7})^{1/2}\simeq 1.069$ at high temperature, and increasing quasilinearly with $1/T$ in the temperature range 4.2–0.5 K (see Appendix B). One can take advantage of this feature to express the right-hand side of (8) as a function of $[nD_{33}(T)]^{-1}$. Using the values of $q(T)$ for $T=4.2$ K and $T=0.56$ K given in Appendix B, one gets

$$\frac{[nD_{33}(0.56\ \mathrm{K})]^{-1}}{[nD_{33}(4.2\ \mathrm{K})]^{-1}}=3.42\pm0.14 . \tag{9}$$

This value is used hereafter to calibrate values of $[nD_{33}(T)]^{-1}$ with respect to its value at $T=4.2$ K. It can also be used to obtain $[nD_{33}(0.56\ \mathrm{K})]^{-1}$ from the values of the same quantity at 4.2 K already published. Taking for instance the result reported by Barbé,[17]

$$[nD_{33}(4.2\ \mathrm{K})]^{-1}=(0.293\pm0.019)\times10^{-18}\ \mathrm{cm\,s} ,$$

one gets

$$[nD_{33}(0.56\ \mathrm{K})]^{-1}=(1.00\pm0.11)\times10^{-18}\ \mathrm{cm\,s} . \tag{10}$$

B. Variation of D^{-1} from 0.56 to 300 K

The cell used in this particular experiment did not contain hydrogen, because it makes optical pumping impossible at room temperature. The measurement gave

$$\frac{[D(0.56\ \mathrm{K})]^{-1}}{[D(300\ \mathrm{K})]^{-1}} = \frac{1.96[nD_{33}(0.56\ \mathrm{K})]^{-1}+0.05[nD_{34}(0.56\ \mathrm{K})]^{-1}}{1.97[nD_{33}(300\ \mathrm{K})]^{-1}+0.98[nD_{34}(300\ \mathrm{K})]^{-1}} \simeq 37.2\pm2.5 . \tag{11}$$

TABLE I. Relative variation of $[nD(T)]^{-1}$ with temperature. Comparison between experiment and theoretical predictions computed from different potentials: LJ (Ref. 5), HFDHE2 (Ref. 6), HFD-B(HE) (Ref. 7), and HFIMD (Ref. 8) (see Appendix A). The "error bar" on the computed values accounts for the uncertainty on the composition of the gaseous phase.

		Numerical predictions			
	Experiment	LJ	HFDHE2	HFD-B(HE)	HFIMD
$\frac{[nD(0.56\ \mathrm{K})]^{-1}}{[nD(4.2\ \mathrm{K})]^{-1}}$	2.27	2.04	2.20	2.28	2.16
Uncertainty	±0.07		±0.04		

TABLE II. Comparison between experimental determinations of $(nD_{33})^{-1}$ at 0.57 K and values computed from various potentials: LJ (Ref. 5), HFDHE2 (Ref. 6), HFD-B(HE) (Ref. 7), and HFIMD (Ref. 8) (see Appendix A). Units are 10^{-18} cm s. Columns a, b, and c contain the values reported, respectively, in Secs. III, IV A, and IV B. The column headings for the numerical values refer to the potentials defined in Appendix A.

Experimental values				Numerical values			
a	b	c	Average	LJ	HFDHE2	HFD-B(HE)	HFIMD
0.92±0.17	0.99±0.11	1.17±0.17	1.03±0.08	0.96	1.10	1.14	1.07

Since $(nD_{33})^{-1}$ and $(nD_{34})^{-1}$ at 300 K have been measured by various authors,[12–15] the result (11) can be used to get another value of $(nD_{33})^{-1}$ at 0.56 K. Taking the result quoted by Barbé *et al.*,[30]

$$[nD_{34}(300\text{ K})]^{-1}=(\tfrac{8}{7})^{1/2}[nD_{33}(300\text{ K})]^{-1}$$
$$=(2.30\pm0.12)\times10^{-20}\text{ cm s}\ , \quad (12)$$

we can reexpress the numerator of the right-hand side of (10) as

$$[nD_{33}(0.56\text{ K})]^{-1}[1.96+0.05q(0.56\text{ K})]$$

Taking from Appendix B the value $q(0.56\text{ K})\simeq1.76$, and the above-quoted values for the diffusion coefficients at 300 K, we get from (11)

$$[nD_{33}(0.56\text{ K})]^{-1}=(1.19\pm0.17)\times10^{-18}\text{ cm s}\ . \quad (13)$$

V. COMPARISON BETWEEN EXPERIMENTAL AND THEORETICAL VALUES FOR $[nD_{33}(0.57\text{ K})]^{-1}$

The three independent experimental results obtained by the methods described, respectively, in Secs. III, IV A, and IV B are compared in Table II with theoretical values computed from different potentials. For that purpose the results (10) and (13), taken at 0.56 K, have been corrected by a small amount (−1.3%) to be comparable to values at 0.57 K. A weighted mean value of those three results is also ncluded. The theoretical values for $[nD_{33}(0.57\text{ K})]^{-1}$ appear to be about 10% higher than the experimental averaged result. They are at the upper limit of the error bar. A discrepancy cannot be claimed definitely, but it would be extremely desirable to reduce experimental errors on the measurements in order to confirm (or deny) this disagreement. It is interesting to point out that a discrepancy of the same order of magnitude exists for the experimental results around 1.5 K reported in Ref. 19. At 4.2 K, the situation is similar. The value quoted above[17] (0.293±0.019) is smaller than those computed either with the LJ potential (0.317×10^{-18} cm s) or with the other potentials ($\simeq0.335$ in units of 10^{-18} cm s).

VI. VARIATIONS OF $(nD_{33})^{-1}$ WITH THE TEMPERATURE

Even when the linear gradients of the magnetic field are canceled, the relaxation of the transverse magnetization represented by the term $1/T_2^0$ in (3) is still mainly due to field inhomogeneities over the cell. Apart from a small contribution of the wall relaxation which can easily be taken into account, $1/T_2^0$ represents the contributions of higher-order gradients. They all scale as diffusion times, i.e., as D^{-1}:

$$\frac{1}{T_2^0}=\frac{\Lambda}{D(T)}\ . \quad (14)$$

The coefficient Λ depends on the geometrical parameters of the cell and on the map of the inhomogeneities of the magnetic field. Provided that Λ is temperature independent (it is a reasonable assumption over the temperature range 0.5–1 K, and we verified that neither the optimal currents in the linear-gradient compensation coils nor the Larmor frequency depends on the temperature), the variations of $1/T_2^0$ reflect directly those of D^{-1}. We used this property to study the variation of D^{-1} with the temperature. The value of Λ can be determined by calibration at 0.56 K on the value of D^{-1} obtained either in Sec. III, or that obtained in Sec. IV A as a function of $[nD_{33}(4.2\text{ K})]^{-1}$. We choose this last alternative because of our large uncertainty on the absolute value of $[nD_{33}(0.57\text{ K})]^{-1}$. Also the theoretical predictions for $[nD_{33}\ (4.2\text{ K})]^{-1}$ are the same for all the potentials considered (except for LJ, which is off by a few percent), whereas they diverge at low temperature. Hence the ratio $[nD_{33}(T)]^{-1}/[nD_{33}(4.2\text{ K})]^{-1}$ is a good parameter to test the temperature dependence of the diffusion coefficient. Performing this measurement for a set of different cells with increasing gaseous densities of ^{3}He and the different cells with increasing gaseous densities of ^{3}He and the same amount of ^{4}He gives $[nD_{33}(T)]^{-1}/[nD_{33}(4.2\text{ K})]^{-1}$ according to formula (1).

The results are reported in Fig. 2. Theoretical values for the ratio $[nD_{33}(T)]^{-1}/[nD_{33}(4.2\text{ K})]^{-1}$ have also been reported for the different available potentials. The observed variation with temperature is quite similar to the computed ones in the range 1–0.5 K. The experimental error does not allow us to discriminate among the potentials, which give a very similar temperature dependence for $[nD_{33}(T)]^{-1}$. Although extending the explored temperature range would have been desirable, our study was limited to the (0.5–1)-K temperature range. Indeed, 0.5 K was the lowest temperature available with our apparatus. But one also expects at lower temperature a contribution to T_2 from the ^{3}He condensed on the walls of the cell. Above 1 K, the ^{4}He coating on the wall becomes too thin, and the contribution to T_2 of the wall re-

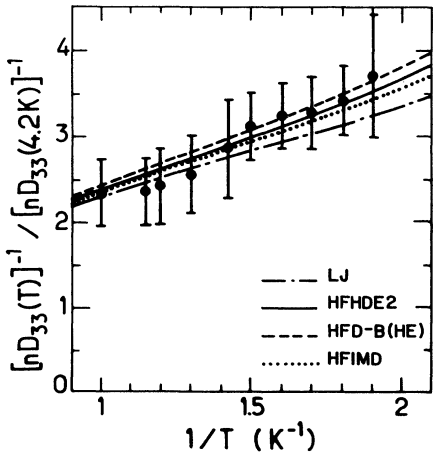

FIG. 2. Relative variations of $[nD_{33}(T)]^{-1}$. The values for $T=4.2$ K are taken as a reference for the experimental points as well as for the theoretical curves computed from various potentials: LJ (Ref. 5), HFDHE2 (Ref. 6), HFD-B (Ref. 7), and HFIMD (Ref. 8) (see Appendix A).

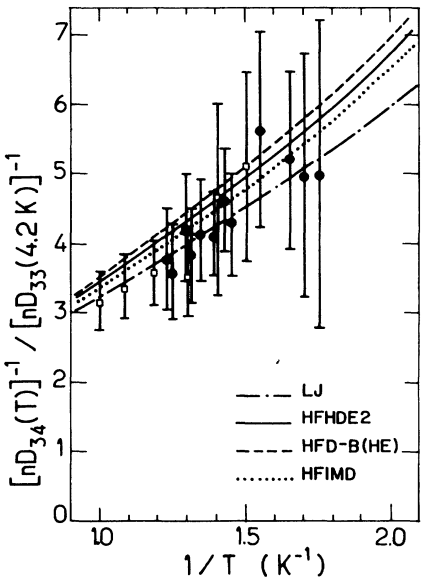

FIG. 3. Relative variations of $[nD_{34}(T)]^{-1}$. Calibration is made on $[nD_{33}(4.2\text{ K})]^{-1}$ for the experimental points as well as for the theoretical curves. The empty squares refer to values obtained by studying, at fixed temperature, the variation of D^{-1} with n_3 according to formula (1). The solid circles refer to direct measurements under SVP conditions for n_4. Numerical predictions have been computed from various potentials: LJ (Ref. 5), HFDHE2 (Ref. 6), HFD-B (Ref. 7), and HFIMD (Ref. 8) (see Appendix A).

laxation cannot be neglected. So at both ends of the temperature range, T_2 measurements would not account only for the diffusion of gaseous ^{3}He.

VII. MEASUREMENT OF $(nD_{34})^{-1}$

As discussed in the preceding sections, the variation of D^{-1} with n_3 gives, according to (1), $n_4(nD_{34})^{-1}$ as the value for $n_3=0$ of the best linear fit to the experimental points (Fig. 1). Knowing the density of ^{4}He, one can obtain $[nD_{34}(T)]^{-1}$ in this way. A few of such measured values have been plotted in Fig. 3 (empty squares). Nevertheless, the precision of these measurements is not very high, especially for the low-temperature points where there is in the gaseous phase much more ^{3}He than ^{4}He. Also, around the dew point, the value to be used for n_4 somewhat depends on the condensation model considered.

For that reason we measured $\Gamma_m(T)$ for a single cell containing only a low ^{3}He density and a large quantity of ^{4}He, so that it is under saturated-vapor conditions in the whole temperature range. n_3 has been chosen equal to $0.14n_0$, and except at the lowest temperature, the ^{3}He contribution to D^{-1} is small. We measured $\Gamma_m(T)$ over the entire temperature range, and using (7), we calibrated Γ_m in terms of the diffusion coefficient at 0.56 K. At that temperature, D^{-1} is equal to

$$[nD_{33}(0.56\text{ K})]^{-1}[n_3+n_4^{\mathrm{SVP}}q(0.56\text{ K})]\ ,$$

where $n_3=0.14n_0$ and $n_4^{\mathrm{SVP}}=0.05n_0$. ^{3}He plays then a dominant role, and it is appropriate to approximate q(0.56 K) by its theoretical value taken in Appendix B. One expresses finally D^{-1} at 0.56 K in terms of $[nD_{33}(4.2\text{ K})]^{-1}$ using formula (9). Experimental points for $[nD_{33}(T)]^{-1}/[nD_{33}(4.2\text{ K})]^{-1}$ obtained in this way are plotted in Fig. 3. An important part of the corresponding error bars comes from the uncertainty on the temperature, which results in a substantial uncertainty on the ^{4}He density n_4^{SVP}. The theoretical curves are well inside those error bars. The available potentials describe correctly the temperature dependence of $[nD_{34}(T)]^{-1}$, as for $[nD_{33}(T)]^{-1}$.

VIII. CONCLUSIONS

First measurements of the diffusion coefficients in ^{3}He gas and the ^{3}He-^{4}He mixture below 1 K have been reported. The absolute values are in rough agreement with the predictions that we have computed from currently used helium-helium potentials. However, as is already the case of higher temperatures, the computed values of the inverse diffusion coefficient seem somewhat too large.

The relative temperature dependence of these coefficients between 4.2 and 0.5 K is rather sensitive to small variations in the low-energy part of the potential. Experimental results fit well with theoretical predictions, but are not sufficiently precise to make a clear discrimination among the various models of the pair potential. However, as it appears in Table I, the crude Lennard-Jones potential[5] seems rather outclassed. More accurate measurements and lower temperature studies would be valuable.

ACKNOWLEDGMENTS

The authors wish to thank Professor J. Brossel for his help and active interest in this work. The Laboratoire de Spectroscopie Hertzienne de l'Ecole Normale Supérieure is "Laboratoire associé au Centre National de la Recherche Scientifique et à l'Université Paris VI."

APPENDIX A: VARIOUS APPROXIMATIONS TO THE INTERATOMIC He-He POTENTIAL

Several determinations for the interatomic potential among ground-state helium atoms have been mentioned in the paper. Their relevant characteristics are listed below.

The Lennard-Jones[5] 12-6 potential (LJ)

$$V(r)=4\epsilon\left[\left[\frac{\sigma}{r}\right]^{12}-\left[\frac{\sigma}{r}\right]^{6}\right],$$

$$\epsilon=10.22\ \text{K},\quad \sigma=2.556\ \text{Å}$$

is used only as a reference because of its simple analytic form.

The Aziz *et al.*[6] HFDHE2 potential (HF is for Hartree-Fock, D for dispersive, HE for helium) is given as:

$$V(r)=\epsilon V^{*}(x),\quad \text{with } x=r/r_m\ ,$$

$$V^{*}(x)=A\exp[h(x)]-F(x)\left[\sum_{j=0}^{2}\frac{C_{2j+6}}{X^{2j+6}}\right],$$

with

$$h(x)=-\alpha x\ ,$$

$$F(x)=\begin{cases}\exp\left[-\left[\dfrac{D}{x}-1\right]^{2}\right] & \text{for } x<D\ ,\\ 1 \quad \text{for } x\geq D\ .\end{cases}$$

The best values fitted on intermediate- and high-temperature experimental data by these authors are

$$A=0.5449\times10^{6}\quad \alpha=13.353,\quad D=1.241\ ,$$

$$C_6=1.373,\quad C_8=0.4254,\quad C_{10}=0.1781\ ,$$

$$\epsilon=10.8\ \text{K},\quad r_m=2.9673\ \text{Å}\ .$$

The HFD-B (HE) potential of Aziz, McCourt, and Wong (β refers to a variant form of the HF part of the potential)[7] is given by the preceding formula, $h(x)$ being replaced by

$$h(x)=-\alpha x+\beta x^{2}\ .$$

The best set of the parameters obtained according to new experimental data is now

$$A=1.884\times10^{5},\quad \alpha=10.433,\quad \beta=-2.2797\ ;$$

$$C_6=1.367,\quad C_8=0.4212,\quad C_{10}=0.1747\ ;$$

$$\epsilon=10.95\ \text{K},\quad r_m=2.963\ \text{Å},\quad D=1.4826\ .$$

The HFIMD potential of Feltgen *et al.*[8] (IMD means intramolecular dispersive), obtained from experiment through an inversion method, has a much more complicated form

$$V(r)=A\exp[h(r)]+B\exp(-br)+\sum_{n=6}^{18}C_n\frac{f_n(r)}{r^{n}}\ ,$$

$$h(r)=Gr+Cr^{2}\ .$$

The "damping function" $f_n(r)$ is given by

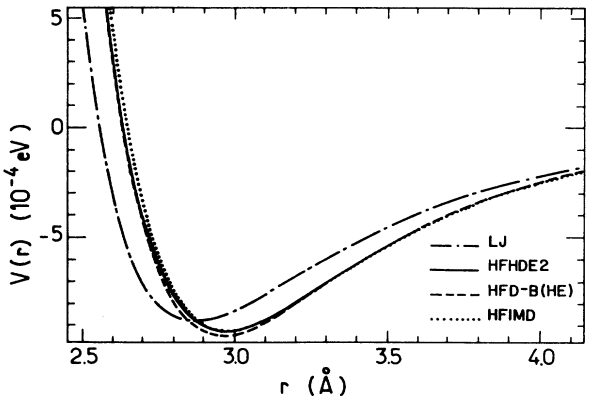

FIG. 4. Various He-He interaction potentials used for the numerical calculations, plotted as a function of the interatomic distance r, in the well region: LJ (Ref. 5), HFDHE2 (Ref. 6), HFD-B (Ref. 7), and HFIMD (Ref. 8) (see Appendix A).

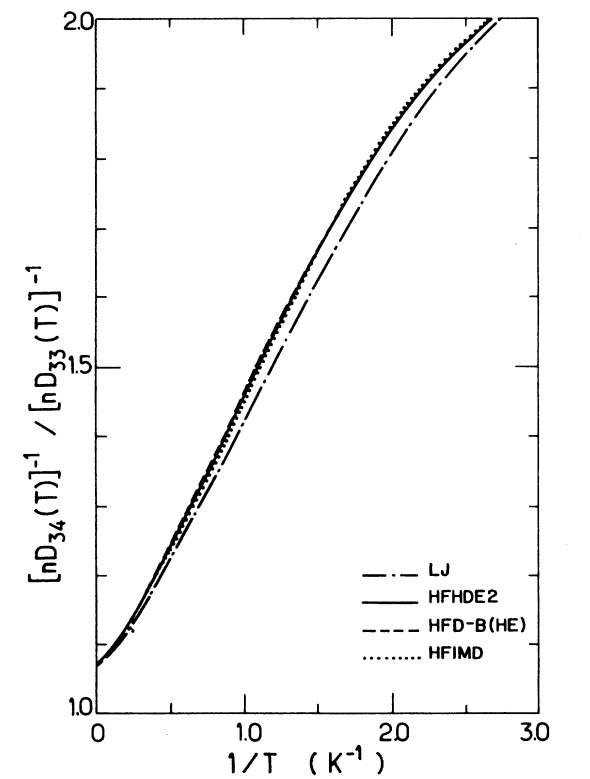

FIG. 5. Temperature dependence of $q(T)=[nD_{34}(T)]^{-1}/[nD_{33}(T)]^{-1}$ computed for the different potentials: LJ (Ref. 5), HFDHE2 (Ref. 6), HFD-B (Ref. 7), and HFIMD (Ref. 8) (see Appendix A). The variation is almost a unique straight line between 4.2 and 0.56 K.

$$f_n(r)=P^2(\nu,\alpha r)+(a\alpha r)^m\exp(-1.4\alpha r) ,$$

with

$$P(\nu,\alpha r)=\frac{1}{\Gamma(\nu)}\int_0^{\alpha r}e^{-t}t^{\nu-1}dr ,$$

$$\nu=1.05n^*+1.24 ,$$

$$a=1.61(n^*)^{-0.911} ,$$

$$m=1.7n^*-1.11 ,$$

$$\alpha r=a_1x[1+\exp(-a_2x)],\quad x=r/r_D,\quad r_D=\sqrt{C_8/C_6} ,$$

and

$$n^*=\begin{cases}n & \text{for } n \text{ even}\\ n-1.378 & \text{for } n \text{ odd} .\end{cases}$$

The values of the parameters come from data inversion and *ab initio* considerations:

$$A=222.6 \text{ eV},\quad G=-3.807 \text{ Å}^{-1},\quad C=-0.129\,55 \text{ Å}^{-2} ,$$

$$b=4.64 \text{ Å}^{-1},\quad a_1=8.5 .$$

The values of dispersion coefficients C_n are (in eV Å^n)

$$C_6=-0.8711,\quad C_8=-2.346,\quad C_{10}=-8.478 ,$$

$$C_{11}=1.096,\quad C_{12}=-42.97,\quad C_{13}=10.41 ,$$

$$C_{14}=-291.4,\quad C_{15}=97.2,\quad C_{16}=-2067 ,$$

$$C_{17}=1090,\quad C_{18}=-288\,10 .$$

A final least-squares fit gives, from ^{3}He and ^{4}He experimental results, $B=36.4$ eV and $a_2=1.458$. Typical variations in the well range of these potentials are shown in Fig. 4.

APPENDIX B: THE RATIO $(nD_{34})^{-1}/(nD_{33})^{-1}$

Figure 5 shows explicitly the temperature dependence of the ratio

$$q(T)=\frac{[nD_{34}(T)]^{-1}}{[nD_{33}(T)]^{-1}} . \tag{B1}$$

Two features should be pointed out. First, for all potentials considered, the numerical values are almost identical down to 0.4 K. Except for the LJ potential, which gives points 1% or 2% lower, all curves are within the thickness of the line. Second, the variation is almost linear in this temperature range, so that $q(T)$ can be approximated by

$$q(T)=1.045+0.395/T , \tag{B2}$$

with a precision better than 2% between 4.2 and 0.57 K. Formula (B2) is only an empirical numerical approximation; the theoretical variation, which involves the ratio of collision integrals,[1] is not so simple.

*Present address: Laboratoire de Physique des Liquides, Université de Paris VI, Tour 16, 4 place Jussieu, 75230 Paris CEDEX 05, France.

[1]C. Lhuiller and F. Laloë, J. Phys. (Paris) **43**, 197 (1982); **43**, 225 (1982); C. Lhuiller, J. Phys. (Paris) **44**, 1 (1983).

[2]G. Tastevin, P.-J. Nacher, M. Leduc, and F. Laloë, J. Phys. Lett. **46**, L249 (1985); M. Leduc, P.-J. Nacher, D. S. Betts, J. M. Daniels, G. Tastevin, and F. Laloë, Europhys. Lett. **4**, 59 (1987).

[3]E. G. D. Cotten, M. J. Offerhaus, and J. de Boer, Physica **20**, 501 (1954).

[4]D. M. Ceperley and H. Partridge, J. Chem. Phys. **84**, 820 (1986); P. G. Burton, Mol. Phys. **58**, 637 (1986). This last reference contains an extensive list of previous works.

[5]J. de Boer and A. Michels, Physica **6**, 409 (1938).

[6]R. A. Aziz, V. P. S. Nain, J. S. Carley, W. L. Taylor, and G. T. McConville, J. Chem. Phys. **70**, 4330 (1979).

[7]R. A. Aziz, F. R. W. McCourt, and C. C. K. Wong, Mol. Phys. **61**, 1487 (1987).

[8]R. Feltgen, H. A. Köhler, H. Pauly, and F. Torello, J. Chem. Phys. **76**, 2360 (1982).

[9]M. Gutowski, J. Verbeek, J. H. Van Lenthe, and G. Chalasinski, Chem. Phys. **111**, 271 (1987).

[10]R. F. Bishop, H. B. Ghassib, and M. R. Strayer, J. Low. Temp. Phys. **26**, 669 (1977).

[11]J. A. Cameron and G. M. Seidel, J. Chem. Phys. **83**, 3621 (1986).

[12]P. J. Bendt, Phys. Rev. **110**, 85 (1958).

[13]G. A. DuBro and S. Weissman, Phys. of Fluids **13**, 2682 (1970).

[14]J. C. Liner and S. Weissman, J. Chem. Phys. **56**, 2288 (1972).

[15]T. R. Marrero and E. A. Mason, J. Chem. Phys. Ref. Data **1**, 3 (1972).

[16]K. Luszczynski, R. E. Norberg, and J. E. Opfer, Phys. Rev. **128**, 186 (1962). Other results from the same authors are quoted in L. Monchick, E. A. Mason, R. J. Munn, and F. J. Smith, Phys. Rev. **139A**, 1076 (1965).

[17]R. Barbé, thèse de doctorat d'état, Université de Paris VI, 1977 (unpublished).

[18]P.-J. Nacher, thèse de doctorat d'état, Université de Paris VI, 1985 (unpublished).

[19]M. Himbert, J. Dupont-Roc, M. Leduc, and P.-J. Nacher, in Proceedings of the 18th International Conference on Low Temperature Physics, Kyoto, 1987 [Jpn. J. of Appl. Phys. **26-3**, CJ01 (1987)].

[20]V. J. Emery, Phys. Rev. **133A**, 661 (1964).

[21]J. O. Hirschfelder, C. F. Curtiss, and R. B. Bird, *Molecular Theory of Gases and Liquids* (Wiley, New York, 1954).

[22]It must be recalled also that formula (2), giving the diffusion coefficient, results from an approximate solution of the Boltzmann equation (Ref. 1). It is generally accepted that formula (2) is correct to within a few percent.

[23]We investigated the uncertainty on the final gas density produced by the sealing process by directly monitoring the pres-

sure in a test cell with a Barocel manometer during the operation. It turns out that the effect is negligible.

[24]F. D. Colegrove, L. D. Schearer, and G. K. Walters, Phys. Rev. **132**, 2561 (1963),

[25]M. Himbert, V. Lefevre-Seguin, P.-J. Nacher, J. Dupont-Roc, M. Leduc, and F. Laloë J. Phys. (Paris) Lett. **44**, L523 (1983).

[26]M. Himbert and J. Dupont-Roc, in *Proceedings of the 17th International Conference on Low Temperature Physics,* edited by U. Eckern, A. Schmid, W. Weber, and H. Wühl (North-Holland, Amsterdam, 1984).

[27]A. Abragam, *Principles of Nuclear Magnetism* (Oxford University Press, Oxford, England, 1961).

[28]V. Lefevre, P.-J. Nacher, and F. Laloë, J. Phys. (Paris) **43**, 89 (1982).

[29]J. Wilks, *The Properties of Liquid and Solid Helium* (Oxford University Press, Oxford, England, 1967).

[30]R. Barbé, M. Leduc, and F. Laloë, J. Phys. (Paris) **35**, 935 (1974).